

# High-efficiency multiplex biallelic heritable editing in *Arabidopsis* using an RNA virus

Ugrappa Nagalakshmi <sup>1,2,\*†</sup> Nathan Meier <sup>1,3</sup> Jau-Yi Liu,<sup>1,3</sup> Daniel F. Voytas <sup>4,5,6</sup> and Savithamma P. Dinesh-Kumar <sup>1,2,3,\*†</sup>

<sup>1</sup> Department of Plant Biology, College of Biological Sciences, University of California, Davis, California, USA

<sup>2</sup> Innovative Genomics Institute, University of California, Berkeley, California, USA

<sup>3</sup> The Genome Center, College of Biological Sciences, University of California, Davis, California, USA

<sup>4</sup> Department of Genetics, Cell Biology and Development, University of Minnesota, St. Paul, Minnesota, USA

<sup>5</sup> Center for Precision Plant Genomics, University of Minnesota, St. Paul, Minnesota, USA

<sup>6</sup> Center for Genome Engineering, University of Minnesota, St. Paul, Minnesota, USA

\*Author for correspondence: [spdineshkumar@ucdavis.edu](mailto:spdineshkumar@ucdavis.edu) (S.P.D.-K.) and [unagalakshmi@ucdavis.edu](mailto:unagalakshmi@ucdavis.edu) (U.N.)

†Senior authors

U.N. and S.P.D.-K. conceptualize the project and designed the experiments. U.N. and J.-Y.L. performed the experiments. U.N. and N.M. analyzed the data and interpreted the results. D.F.V. provided suggestions and discussed the results with S.P.D.-K. U.N., N.M., and S.P.D.-K. wrote the original draft of the manuscript. All authors reviewed and edited the manuscript.

The author responsible for distribution of materials integral to the findings presented in this article in accordance with the policy described in the Instructions for Authors (<https://academic.oup.com/plphys/pages/General-Instructions>) is: Savithamma P. Dinesh-Kumar ([spdineshkumar@ucdavis.edu](mailto:spdineshkumar@ucdavis.edu)).

Dear Editor,

Genome editing technology is being rapidly adopted for gene function studies in plants (Gao, 2021). The delivery of the Cas (CRISPR-associated) nucleases and single-guide RNAs (sgRNAs) into plant cells is commonly accomplished by *Agrobacterium*-mediated transformation. Although *Arabidopsis* (*Arabidopsis thaliana*) is easy to transform, the generation of biallelic-edited plants requires screening of many plants in subsequent generations. Here, we describe the optimization of an engineered *Tobacco rattle virus* (TRV)-based vector for in planta delivery of sgRNAs fused to tRNA isoleucine sequence (sgRNA-tRNA<sup>Ileu</sup>) that can induce efficient multiplex somatic and biallelic heritable editing in a single generation in *Arabidopsis* that express *SpCas9*.

Recently, we demonstrated that sgRNA fused to tRNA isoleucine (tRNA<sup>Ileu</sup>) moves efficiently and induces high efficiency heritable editing in *SpCas9* expressing transgenic *Nicotiana benthamiana* (Ellison et al., 2020). Therefore, we tested editing in *Arabidopsis* using TRV with sgRNA targeted to *PHYTOENE DESATURASE3* (*AtPDS3*) fused to tRNA<sup>Ileu</sup> (Supplemental Figure S1). *Agrobacterium* harboring TRV1 and TRV2::sgRNA<sup>AtPDS3</sup>-tRNA<sup>Ileu</sup> were delivered into Col-0 expressing *SpCas9* (Col-0::*SpCas9*) by syringe

infiltration of leaves, agro-pricking, and agro-flooding methods (see Supplemental Text S1 for details) (Supplemental Figure S2). About 3% (1/36) and 8% (3/36) of the plants showed photobleached regions on the systemic leaves with leaf infiltration and agro-pricking methods, respectively (Supplemental Figure S3A). With agro-flooding, about 22% of the plants (8/36) showed the photobleaching phenotype (Supplemental Figure S3B) indicating that the agro-flooding is more efficient for sgRNA delivery into *Arabidopsis*.

In *N. benthamiana*, sgRNA fused to *Arabidopsis Flowering Locus T* without the start codon (*mAtFT*) and tRNA methionine (tRNA<sup>Met</sup>) also facilitate efficient TRV movement (Ellison et al., 2020). Therefore, we evaluated the movement of TRV with sgRNA<sup>AtPDS3</sup> fused to *mAtFT* and tRNA<sup>Met</sup> (Supplemental Figure S1) in *Arabidopsis* using agro-flooding method. A substantially higher amount of virus was detected in systemic leaves of TRV2::sgRNA<sup>AtPDS3</sup>-tRNA<sup>Ileu</sup> infected plants compared with sgRNA<sup>AtPDS3</sup> fused to *mAtFT*, tRNA<sup>Met</sup>, or sgRNA<sup>AtPDS3</sup> alone (Figure 1A) indicating that the tRNA<sup>Ileu</sup> facilitates better TRV movement in *Arabidopsis*. This contradicts our recent report that both tRNA<sup>Ileu</sup> and *mAtFT* promote better TRV movement in *N. benthamiana* (Ellison et al., 2020). We presume this is

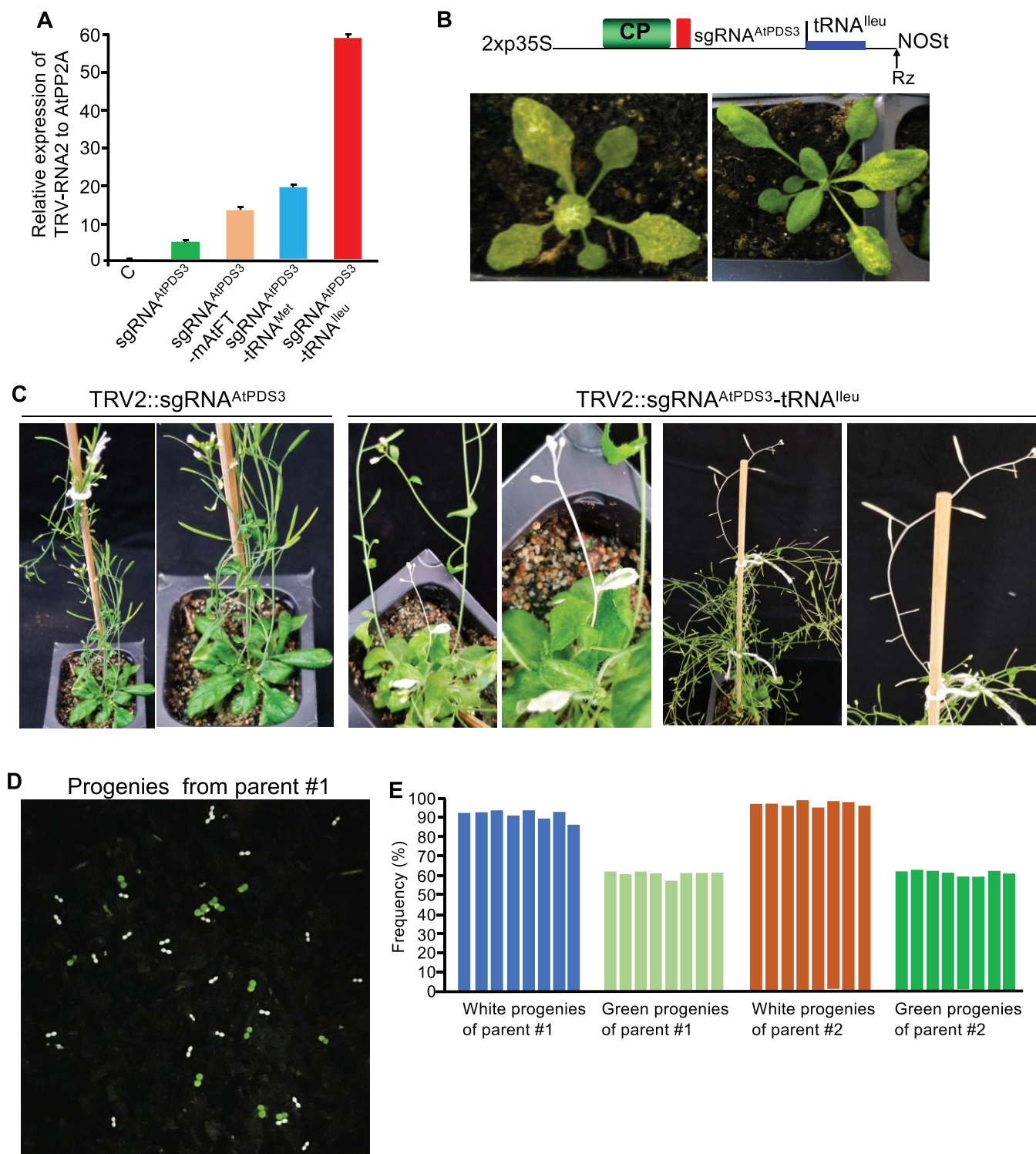


**Figure 1** Efficient somatic and heritable editing in *AtPDS3* using TRV with tRNA<sup>lleu</sup>. A, The inclusion of tRNA<sup>lleu</sup> in TRV promotes enhanced systemic movement. Comparison of systemic movement of TRV with indicated sequences. Relative levels of TRV RNA2 were measured by reverse transcription quantitative PCR (RT-qPCR) using *PROTEIN PHOSPHATASE 2A* (*AtPP2A*) as a reference. Data from three replicates were combined and values are shown as mean  $\pm$  sd. C, Mock-treated Col-0. B, Schematic of TRV RNA2 vector with sgRNA<sup>AtPDS3</sup> fused to tRNA<sup>lleu</sup> (top) and plant phenotype (bottom). White photobleached regions on the leaves indicate loss of *AtPDS3* function. 2  $\times$  p35S, duplicated *Cauliflower mosaic virus* (CaMV) 35S promoter; CP, coat protein; Rz, self-cleaving ribozyme; NOST, nopaline synthase terminator. C, White photobleaching phenotype in some cauline leaves, stem and flowers (middle panels), and in siliques (right panels) of plants infected with TRV1 + TRV2::sgRNA<sup>AtPDS3</sup>-tRNA<sup>lleu</sup> compared with TRV1 + TRV2::sgRNA<sup>AtPDS3</sup> (left panels). The right panel in each group is an enlarged version of part of the left panel. D, The phenotype of M1 progenies of seeds collected from a parental plant infected with TRV1 + TRV2::sgRNA<sup>AtPDS3</sup>-tRNA<sup>lleu</sup>. White photobleached seedlings are indicative of biallelic editing and loss of *AtPDS3* function. E, Indel mutation frequencies in selected eight white and eight green progenies from two parents assessed by NGS of amplicons spanning the *AtPDS3* target site.

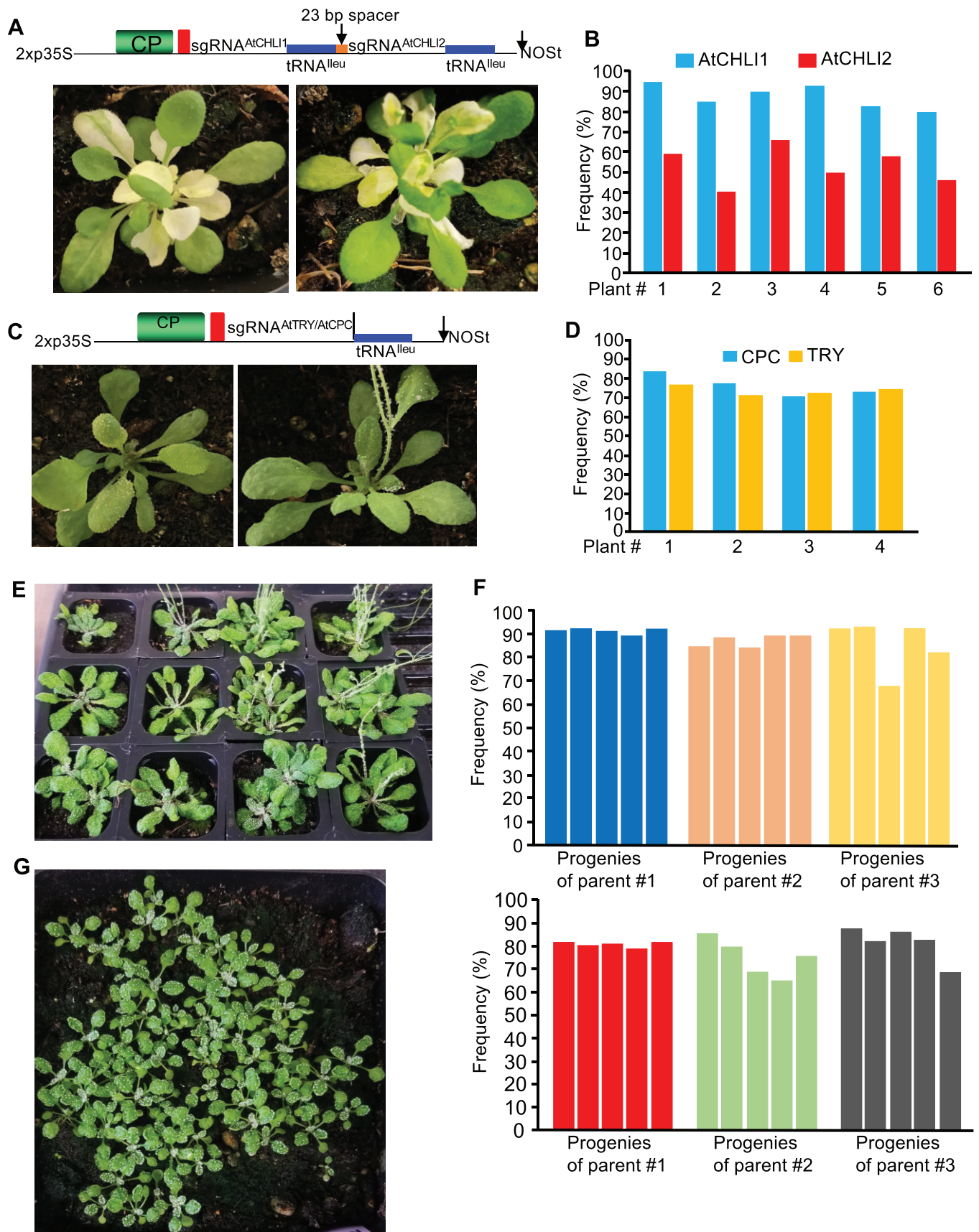


**Figure 2** Efficient multiplex somatic and heritable editing using TRV augmented with tRNA<sup>leu</sup>. A, Schematic of TRV RNA2 vector with sgRNA<sup>AtCHLI1</sup> and sgRNA<sup>AtCHLI2</sup> fused to tRNA<sup>leu</sup> with a 23-bp spacer (top) and plant phenotype (bottom). White albino and yellow leaves indicate editing and loss of function of both *AtCHLI2* and *AtCHLI1*. 2 × p35S, duplicated *Cauliflower mosaic virus* (CaMV) 35S promoter; CP, coat protein

(continued)

because the AtFT protein is the mobile form and not the AtFT mRNA in Arabidopsis (Corbesier et al., 2007; Jaeger and Wigge, 2007).

In the agro-flooded Col-0::SpCas9 plants with TRV2::sgRNA<sup>AtPDS3</sup>-tRNA<sup>lleu</sup>, we not only observed photobleaching phenotype in leaves (Figure 1B) but also in some of the rosette and cauline leaves as well as the siliques and seed pods (Figure 1C and Supplemental Figure S4). Sanger sequencing followed by ICE analysis (<https://ice.synthego.com/#/>) (Hsiau et al., 2019) of PCR-amplified products spanning the target site using DNA extracted from the photobleached leaves in Figure 1B confirmed the mutations in the AtPDS3 (Supplemental Figure S3C). We also estimated the somatic editing by analyzing leaf tissue from completely photobleached regions, regions with overlapping photobleached and green (referred to as mosaic regions) and the green regions from plants showing photobleaching (Figure 1B). The editing efficiency was 60%–99% in the completely photobleached regions, 20%–70% in the mosaic regions, and 0%–26% in the green regions (Supplemental Figure S5).

Next, we assessed the heritability of AtPDS3 editing by collecting seeds from the aforementioned parent plants in three batches between principal growth stage 8–5 days after principal growth stage 6.9 (Boyes et al., 2001) that we refer to here as early-, middle-, and late-stage developed seeds. We observed a few photobleached seedlings from late-stage developed seeds. From the middle-stage, 39%–60% of the progeny seedlings were completely photobleached, indicating biallelic mutations in AtPDS3 compared with about 4–6% in TRV2 with sgRNA<sup>AtPDS3</sup> alone (Figure 1D and Supplemental Figure S6A and B). Next-generation sequencing (NGS) of the amplicons of the progeny white seedlings from two parents showed indel frequencies ranging from 86% to 93% and 95% and 99% (Figure 1E and Supplemental Table S1). In green seedlings, indel frequency ranged from 57% to 62% (Figure 1E and Supplemental Table S2). Sanger sequencing and ICE analysis of white progeny seedlings from two additional parents showed indel frequencies of 88%–99% and 93%–99% (Supplemental Figure S6C). We also tested whether TRV is transmitted to the mutant progeny by RT-PCR and found no evidence for the virus in the progenies (Supplemental Figure S7). These results indicate that TRV2::sgRNA<sup>AtPDS3</sup>-tRNA<sup>lleu</sup> induces high-efficiency somatic and heritable editing in Arabidopsis.

To test the feasibility of multiplex editing, we targeted *Magnesium-chelatase subunit 1* (AtCHL1) and *Magnesium-chelatase subunit 2* (AtCHL2) involved in chlorophyll synthesis. For this, we generated TRV2 with two sgRNAs that target both genes in tandem with a 23-base pair spacer (Figure 2A). The TRV2::sgRNA<sup>AtCHL1</sup>-tRNA<sup>lleu</sup>-S-sgRNA<sup>AtCHL2</sup>-tRNA<sup>lleu</sup>-infected plants exhibited a yellow or white leaf color phenotype starting 15–20 days post-transplanting after agro-flooding (Figure 2A and Supplemental Figure S8). NGS of the amplicons detected indel frequencies of 79%–94% in AtCHL1 and 45%–66% in AtCHL2 (Figure 2B and Supplemental Tables S3 and S4). We were unable to estimate the heritability of multiplex editing because the parent plants showing phenotypes produced very few seeds and most of the progeny resulting from these seeds died.

To assess the heritability of multiplex editing, we targeted *TRIPTYCHON* (AtTRY) and *CAPRICE* (AtCPC), which function as negative regulators of trichome development and display increased trichomes on leaves of double mutants, leading to a clustered leaf trichomes phenotype (Schellmann et al., 2002; Wang et al., 2015). We introduced TRV1 and TRV2 with a sgRNA fused tRNA<sup>lleu</sup> that targets both AtTRY and AtCPC (TRV2::sgRNA<sup>AtTRY/AtCPC</sup>-tRNA<sup>lleu</sup>) (Figure 2C) by agro-flooding into Col-0::SpCas9 plants. Clustered trichomes on the leaves and the stems were visible in plants approximately 15–20 days post-transplanting (Figure 2C and Supplemental Figure S9A). The somatic editing frequencies ranged from 70% to 83% in the AtCPC and 71% to 76% in the AtTRY (Figure 2D and Supplemental Tables S5 and S6). In the next generation, about 12%–38% of the progeny plants exhibited the clustered leaf trichomes (Figure 2E and Supplemental Figure S9B and C). The NGS of the amplicon of progenies from three different parents detected indel frequencies ranging from 89% to 92%, 84% to 89%, and 68% to 93% in the AtCPC gene (Figure 2F, top panel and Supplemental Table S7) and 79% to 82%, 65% to 86%, and 69% to 88% in the AtTRY gene (Figure 2F, bottom panel and Supplemental Table S8). Furthermore, 100% of the M2 progenies displayed the clustered leaf trichomes (Figure 2G and Supplemental Figure S9D). Thus, TRV with tRNA<sup>lleu</sup> induces highly efficient multiplex heritable knockout mutations in Arabidopsis.

The optimized and simple agro-flooding method combined with TRV augmented with tRNA<sup>lleu</sup> described here is very efficient for inducing somatic and heritable multiplex editing in SpCas9 expressing Arabidopsis. Biallelic mutants can be

#### Figure 2 (Continued)

parent; Rz, self-cleaving ribozyme; and NOS<sub>t</sub>, nopaline synthase terminator. B, Indel mutation frequencies in AtCHL1 and AtCHL2 from six independent plants showing albino and yellow leaves phenotype. C, Schematic of TRV RNA2 vector with sgRNA targeting both AtTRY and AtCPC fused to tRNA<sup>lleu</sup> (top) and plant phenotype (bottom). Trichomes on the leaves and stems are due to editing and loss-of-function of both AtTRY and AtCPC. D, Indel mutation frequencies in AtTRY and AtCPC from four independent parent plants showing leaf trichome phenotype. E, The phenotype of M1 progenies of seeds collected from a parental plant infected with TRV1 + TRV2::sgRNA<sup>AtTRY/AtCPC</sup>-tRNA<sup>lleu</sup>. Trichomes on leaves and stems are indicative of biallelic editing in both AtTRY and AtCPC. F, Indel mutation frequencies in five M1 progenies of three independent parent plants were assessed by NGS of amplicons spanning the AtCPC (top panel) and AtTRY (bottom panel) target sites. G, The phenotype of M2 progenies of seeds collected from an M1 progeny. All progenies showed leaf trichome phenotype.

generated in a single generation and it also facilitates uncovering lethal phenotypes because the phenotype is visible in the original virus-infected plants. Although TRV can transiently invade the meristem (Martin-Hernandez and Baulcombe, 2008), the addition of tRNA<sup>leu</sup> is essential to achieve efficient heritable editing in *N. benthamiana* (Ellison et al., 2020) and in *Arabidopsis* (this report). Enhanced systemic movement facilitated by tRNA<sup>leu</sup> perhaps leads to more virus invading into the meristem which, in turn, promotes editing in higher numbers of germline cells. In summary, the engineered TRV is an efficient viral vector for gene editing in *N. benthamiana* (Ellison et al., 2020); and gene (this report) and epigenetic (Ghoshal et al., 2020) editing in *Arabidopsis*.

## Supplemental data

**Supplemental Figure S1.** Schematic representation of TRV1, TRV2, and various TRV2 derivative vectors.

**Supplemental Figure S2.** Different methods of introducing TRV vectors with sgRNAs into *Arabidopsis*.

**Supplemental Figure S3.** Somatic editing in *AtPDS3* using TRV augmented with tRNA<sup>leu</sup>.

**Supplemental Figure S4.** Photobleaching of stems, flowers, and siliques of plants infected with TRV expressing sgRNA<sup>AtPDS3</sup> fused to tRNA<sup>leu</sup>.

**Supplemental Figure S5.** Mutation types and editing frequencies in *AtPDS3* in somatic tissue.

**Supplemental Figure S6.** Heritable editing phenotype of *AtPDS3* in M1 progenies.

**Supplemental Figure S7.** TRV is not detected in M1 mutant progenies.

**Supplemental Figure S8.** Plants showing *AtCHL1* and *AtCHL2* somatic editing phenotype.

**Supplemental Figure S9.** Somatic and heritable editing phenotype of *AtTRY* and *AtCPC*.

**Supplemental Table S1.** Mutation types and frequencies of M1 photobleached progenies from two parental plants infected with TRV1 + TRV2::sgRNA<sup>AtPDS3</sup>-tRNA<sup>leu</sup>.

**Supplemental Table S2.** Mutation types and frequencies of M1 green progenies from two parental plants infected with TRV1 + TRV2::sgRNA<sup>AtPDS3</sup>-tRNA<sup>leu</sup>.

**Supplemental Table S3.** Mutation types and frequencies in *AtCHL1* of parental plants infected with TRV1 + TRV2::sgRNA<sup>AtCHL1</sup>-tRNA<sup>leu</sup>-23bp-sgRNA<sup>AtCHL2</sup>-tRNA<sup>leu</sup>.

**Supplemental Table S4.** Mutation types and frequencies in *AtCHL2* of parental plants infected with TRV1 + TRV2::sgRNA<sup>AtCHL1</sup>-tRNA<sup>leu</sup>-23bp-sgRNA<sup>AtCHL2</sup>-tRNA<sup>leu</sup>.

**Supplemental Table S5.** Mutation types and frequencies in *AtCPC* of parental plants infected with TRV1 + TRV2::sgRNA<sup>AtTRY/AtCPC</sup>-tRNA<sup>leu</sup>.

**Supplemental Table S6.** Mutation types and frequencies in *AtTRY* of parental plants infected with TRV1 + TRV2::sgRNA<sup>AtTRY/AtCPC</sup>-tRNA<sup>leu</sup>.

**Supplemental Table S7.** Mutation types and frequencies in *AtCPC* of M1 progenies from three parental plants infected with TRV1 + TRV2::sgRNA<sup>AtTRY/AtCPC</sup>-tRNA<sup>leu</sup>.

**Supplemental Table S8.** Mutation types and frequencies in *AtTRY* of M1 progenies from three parental plants infected with TRV1 + TRV2::sgRNA<sup>AtTRY/AtCPC</sup>-tRNA<sup>leu</sup>.

**Supplemental Table S9.** Oligonucleotides used for cloning target sites, Sanger sequencing, and NGS amplicon sequencing.

**Supplemental Text S1.** Materials and methods.

## Acknowledgments

We thank Professor Jen Sheen and Dr. Jian-Feng Li for providing *SpCas9* expressing *Arabidopsis* line. We also thank April DeMell for critical reading and editing the manuscript and Neha Dinesh-Kumar for editing.

## Funding

This work was supported by Innovative Genomics Institute (IGI; to S.P.D.-K. and U.N.), Agricultural Innovation through Gene Editing program grant no. 2020-67013-31544/project accession no. 1022332 from the USDA National Institute of Food and Agriculture (USDA-NIFA; to S.P.D.-K. and U.N.), and grant no. HR0011-17-2-0053 from the Defense Advanced Research Projects Agency (DARPA; to S.P.D.-K. and D.F.V.).

*Conflict of interest statement.* None declared.

## References

- Boyes DC, Zayed AM, Ascenzi R, McCaskill AJ, Hoffman NE, Davis KR, Gorchach J (2001) Growth stage-based phenotypic analysis of *Arabidopsis*: a model for high throughput functional genomics in plants. *Plant Cell* **13**: 1499–1510
- Corbesier L, Vincent C, Jang S, Fornara F, Fan Q, Searle I, Giakountis A, Farrona S, Gissot L, Turnbull C, et al. (2007) FT protein movement contributes to long-distance signaling in floral induction of *Arabidopsis*. *Science* **316**: 1030–1033
- Ellison EE, Nagalakshmi U, Gamo ME, Huang PJ, Dinesh-Kumar S, Voytas DF (2020) Multiplexed heritable gene editing using RNA viruses and mobile single guide RNAs. *Nat Plants* **6**: 620–624
- Gao C (2021) Genome engineering for crop improvement and future agriculture. *Cell* **184**: 1621–1635
- Ghoshal B, Vong B, Picard CL, Feng S, Tam JM, Jacobsen SE (2020) A viral guide RNA delivery system for CRISPR-based transcriptional activation and heritable targeted DNA demethylation in *Arabidopsis thaliana*. *PLoS Genet* **16**: e1008983
- Hsiao T, Conant D, Rossi N, Maures T, Waite K, Yang J, Joshi S, Kelso R, Holden K, Enzmann BL, et al. (2019) Inference of CRISPR Edits from Sanger Trace Data. *bioRxiv* doi: <https://doi.org/10.1101/251082>
- Jaeger KE, Wigge PA (2007) FT protein acts as a long-range signal in *Arabidopsis*. *Curr Biol* **17**: 1050–1054
- Martin-Hernandez AM, Baulcombe DC (2008) Tobacco rattle virus 16-kilodalton protein encodes a suppressor of RNA silencing that allows transient viral entry in meristems. *J Virol* **82**: 4064–4071
- Schellmann S, Schnittger A, Kirik V, Wada T, Okada K, Beermann A, Thumfahrt J, Jurgens G, Hulskamp M (2002) TRIPTYCHON and CAPRICE mediate lateral inhibition during trichome and root hair patterning in *Arabidopsis*. *EMBO J* **21**: 5036–5046
- Wang ZP, Xing HL, Dong L, Zhang HY, Han CY, Wang XC, Chen QJ (2015) Egg cell-specific promoter-controlled CRISPR/Cas9 efficiently generates homozygous mutants for multiple target genes in *Arabidopsis* in a single generation. *Genome Biol* **16**: 144